Tribol Lett (2008) 32:143–151
DOI 10.1007/s11249-008-9371-9

ORIGINAL PAPER

Nano/Microtribological Properties of Ultrathin Functionalized Imidazolium Wear-Resistant Ionic Liquid Films on Single Crystal Silicon

Yufei Mo · Wenjie Zhao · Min Zhu · Mingwu Bai

Received: 20 June 2008 / Accepted: 22 September 2008 / Published online: 7 October 2008

Abstract Ionic liquids (ILs) are considered as a new kind of lubricant for micro/nanoelectromechanical system (M/NEMS) due to their excellent thermal and electrical conductivity. However, so far, only few reports have investigated the tribological behavior of molecular thin films of various ILs. Evaluating the nanoscale tribological performance of ILs when applied as a few nanometers-thick film on a substrate is a critical step for their application in MEMS/NEMS devices. To this end, four kinds of ionic liquid carrying methyl, hydroxyl, nitrile, and carboxyl group were synthesized and these molecular thin films were prepared on single crystal silicon wafer by dip-coating method. Film thickness was determined by ellipsometric method. The chemical composition and morphology were characterized by the means of multi-technique X-ray photoelectron spectrometric analysis, and atomic force microscopic (AFM) analysis, respectively. The nano- and microtribological properties of the ionic liquid films were investigated. The morphologies of wear tracks of IL films were examined using a 3D non-contact interferometric microscope. The influence of temperature on friction and adhesion behavior at nanoscale, and the effect of sliding frequency and load on friction coefficient, load bearing capacity, and anti-wear durability at microscale were studied. Corresponding tribological mechanisms of IL films were investigated by AFM and ball-on-plane microtribotester. Friction reduction, adhesion resistance, and durability of IL films were dependent on their cation chemical structures, wettability, and ambient environment.

Keywords Ionic liquid · Lubricant · Thin film · Atomic force microscopy · Friction · Wear

Y. Mo · W. Zhao · M. Zhu · M. Bai (✉)
State Key Laboratory of Solid Lubrication, Lanzhou Institute of Chemical Physics, Chinese Academy of Sciences, Lanzhou 730000, China
e-mail: mwbai@lzb.ac.cn

Y. Mo · W. Zhao · M. Zhu
Graduate School of Chinese Academy of Sciences, Beijing 100039, China
e-mail: nanolab@lzb.ac.cn

1 Introduction

The micro/nanoelectromechanical systems (MEMS/NEMS) have obtained rapid development in the past decades due to their superior performance and low unit cost [1]. The commercialization of products based on MEMS and NEMS relies on a better understanding of various devices. Adhesion, friction at nanometer size scale became critical and can be detrimental to the efficiency, power output, and reliability of MEMS/NEMS devices [2]. For example, adhesion is a major cause of the failure of accelerometer used in automobile air bag triggering mechanisms [3] and in digital micromirror displayer [4]. In order to improve tribological performance, lubricants are applied to the MEMS/NEMS device surfaces. The ideal lubricant should be molecularly thick, easy to be applied, highly durable, and insensitive to environment [5].

Ionic liquids (ILs) are synthetic salt with a melting point below 100 °C. Room temperature ionic liquids (RTILs) are synthetic salt with a melting points at or below room temperature. At least one ion has a delocalized charge such that the formation of a stable crystal lattice is prevented and ions are held together by strong electrostatic forces. The ionic liquids were initially developed for use as electrolytes in batteries and for electrodeposition. Recently, ionic liquids are being employed as green solvents for wide

range of synthesis, catalysis, electrochemistry, and liquid–liquid extractions [6–10].

Ionic liquids are considered as potential lubricants. Their strong electrostatic bonding compared to covalently bonded fluids, leads to very desirable lubrication properties. They also possess desirable properties such as negligible volatility, non-flammability, high thermal stability or high decomposition temperature, efficient heat transfer properties, low melting points, as well as compatibility with lubricant additives [11–18]. Unlike conventional lubricants that are electrically insulating, ionic liquids can minimize the contact resistance between sliding surfaces because they are conducting, and conducting lubricants are needed for various electrical applications [19]. In addition, ILs have high thermal conductivity which help to dissipate heat during sliding [20]. The use of ionic liquids instead of hydrocarbon base oil has potential to dramatically reduce air emissions. Perfluoropolyethers (PFPEs) are used in magnetic rigid disk and vacuum grease applications due to their high thermal stability and extremely low vapor pressure [21]. However, PFPEs are often out of action due to degradation catalyzed by strong nucleophilic agents and strong electropositive metals [22, 23], which together with the high cost of PFPEs can limit the application of PFPEs in some fields. From the commercial standpoint, ionic liquids are cheaper than PFPEs, providing the motivation for comparing the tribological properties of the former with latter [24]. ILs are being considered for MEMS/NEMS applications because of their high temperature stability, electrical conductivity, and desirable lubrication properties.

In this study, AFM-based adhesion, friction measurements are presented for silicon substrate coated with the ionic liquids of interest. A friction force microscopy (FFM) was employed to investigate the interfacial structure and tribological properties of thin IL films. A glass sphere probe was used instead of normal silicon nitride probes to reduce the contact pressures produced by sharper silicon nitride tips. Conventional ball-on-flat data are used in conjunction with FFM experiments in order to compare friction and wear properties at micro- and nanoscale.

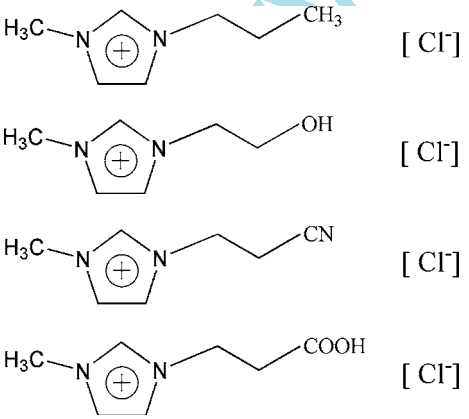

Fig. 1 Chemical structures of MIMCH-CL, MIMOH-CL, MIMCN-CL, and MIMCOOH-CL molecules

2 Experimental

2.1 Materials and Sample Preparation

Polished and cleaned single-crystal silicon (100 P-doped) wafers, obtained from GRINM Semiconductor Materials Co., Ltd. Beijing, were used as substrates for all the data presented in this work. Silicon substrates with dimensions of $10 \times 10 \times 0.5$ mm^3 were cut from Si wafers. The wafers were ultrasonicated in acetone followed by isopropanol for 5 min each. Silicon wafers were treated in freshly prepared Piranha solution (volume ratio 7:3 of 98% H_2SO_4 and 30% H_2O_2) at 90 °C for 30 min to get a hydroxyl-terminated surface.

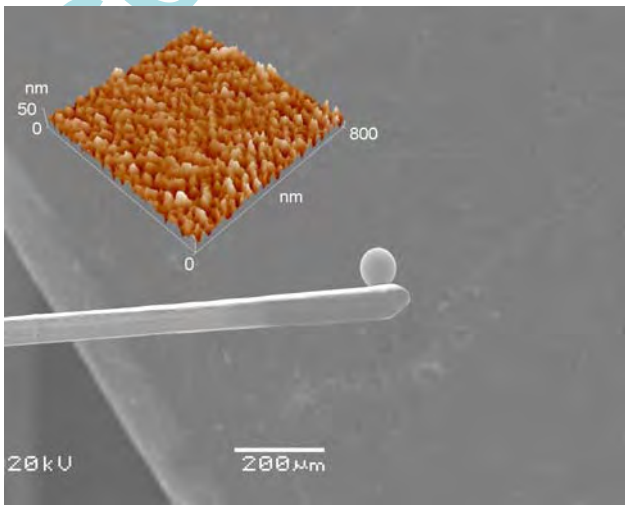

Fig. 2 SEM image of the colloidal probe and AFM topographics of the spherical tip surface

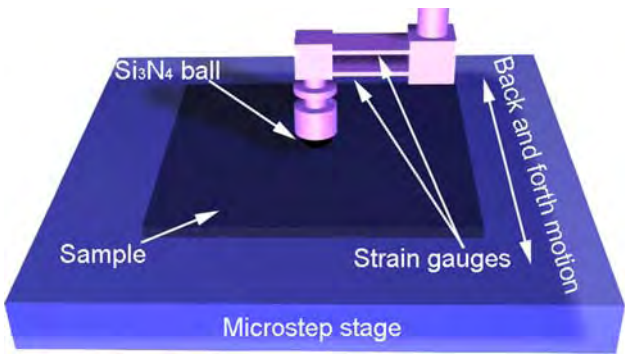

Fig. 3 Schematic illustration of pin-on-plate tribometer

The ionic liquids used in this study are 1-propyl-3-methylimidazolium chloride, 1-ethanol-3-methylimidazolium chloride, 1-propionitrilel-3-methylimidazolium chloride, and 1-propionic acid-3-methylimidazolium chloride abbreviated as MIMCH-CL, MIMOH-CL, MIMCN-CL, and MIMCOOH-CL, respectively. Their molecular structures are schematically shown in Fig. 1. The lubricants were applied on single crystal silicon using dip-coating technique. The dip-coating procedure is as follows. The silicon wafers were pulled from solution with the aid of the motorized stage set at a constant speed of 60 μm/s to obtain films of desired thickness. The solution of ionic liquids in ethanol with an appropriate concentration was dip-coated onto pretreated silicon substrates and then dried at 90 °C for 10 min. The thicknesses of the films after dip-coating were measured by the ellipsometric method. All

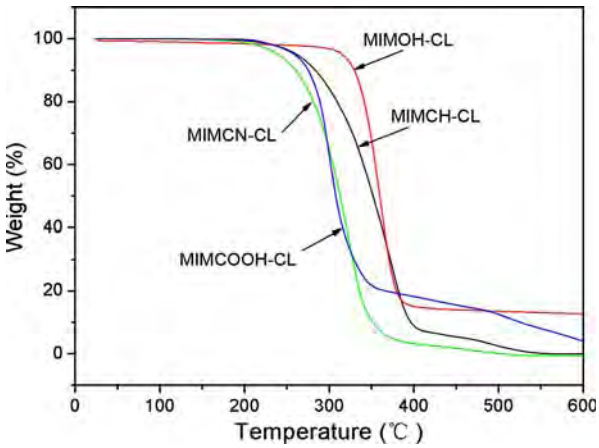

Fig. 4 TGA curves of MIMCH-CL, MIMOH-CL, MIMCN-CL, and MIMCOOH-CL ionic liquids

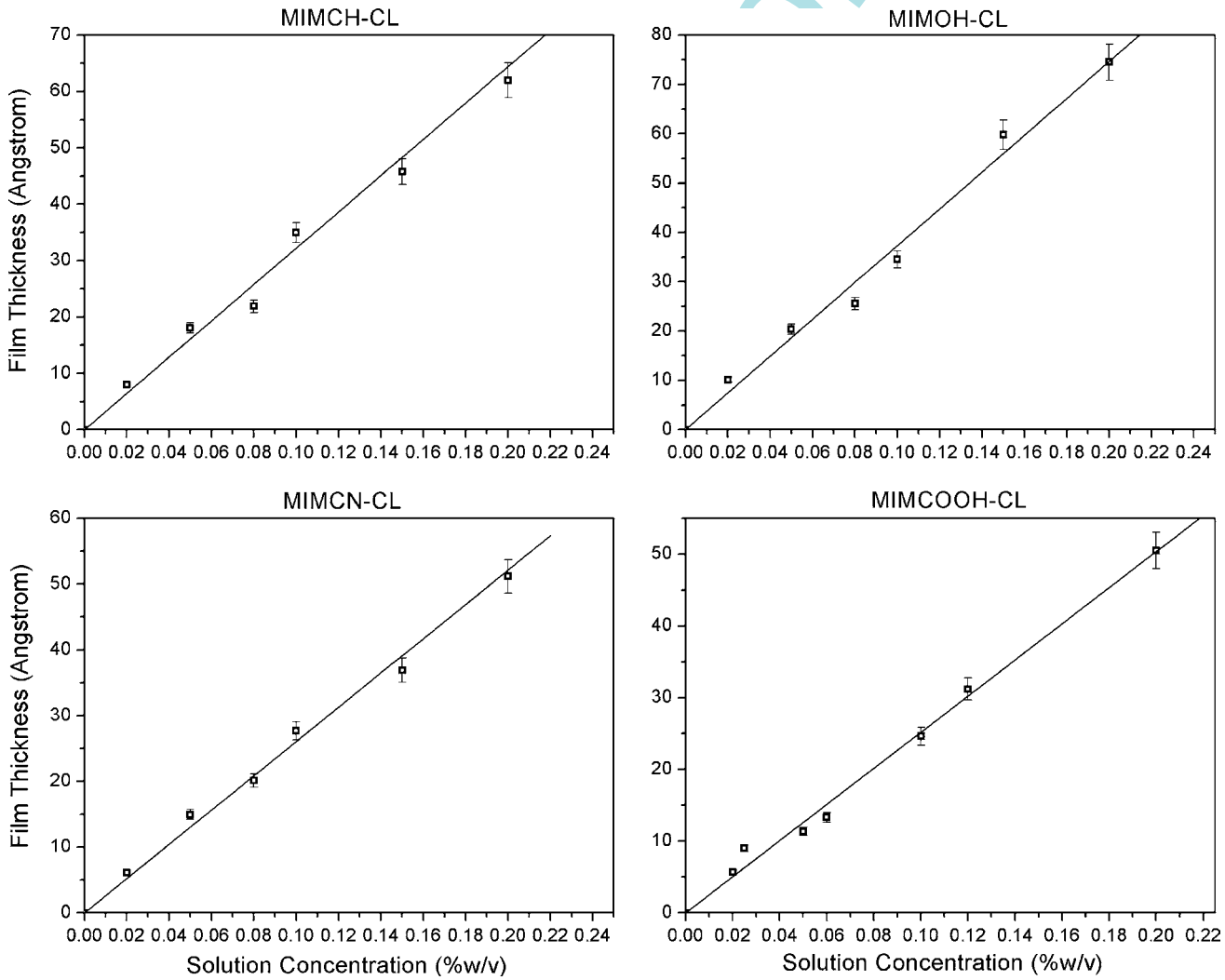

Fig. 5 Plot of film thickness as function of ionic liquid solution concentration at a pull-off velocity of 60 μm/s

procedures were carried out in a class-10 clean room at a humidity of 15% RH and temperature of 20 °C.

2.2 Nanoscale Adhesion, Friction Measurements

Adhesion and friction force measurements were carried out using a commercial CSPM 4000 AFM/LFM microscopy at ambient conditions (20 °C, 15% RH). A colloidal probe was prepared by gluing glass sphere with a radius of 37.5 μm onto a tipless cantilever (normal force constant 2 N/m). The colloidal probe is shown in Fig. 2. From the inset, the three-dimensional surface topography of the top of ball can be seen. The colloidal probe was cleaned by ethanol and then by acetone before use. For all experiments the same cantilever was used in this comparative study. Furthermore, to avoid influence of molecules which may transfer to tip on the FFM experiments, the colloidal probe was scanned on cleaved mica surface to remove physically adsorbed molecules.

Commercially available rectangle Si_3N_4 cantilevers with normal force constant, 0.4 N/m, radius of about 10 nm, and backside coated by gold (Budgetsensors Instruments Inc) were employed. The force distance curves were recorded and the pull-off force reckoned as the adhesive force, which was given by $F = K_c Z_p$, where K_c is the force constant of cantilever and Z_p is the vertical displacement of the piezotube, i.e., the deflection of the cantilever [25, 26].

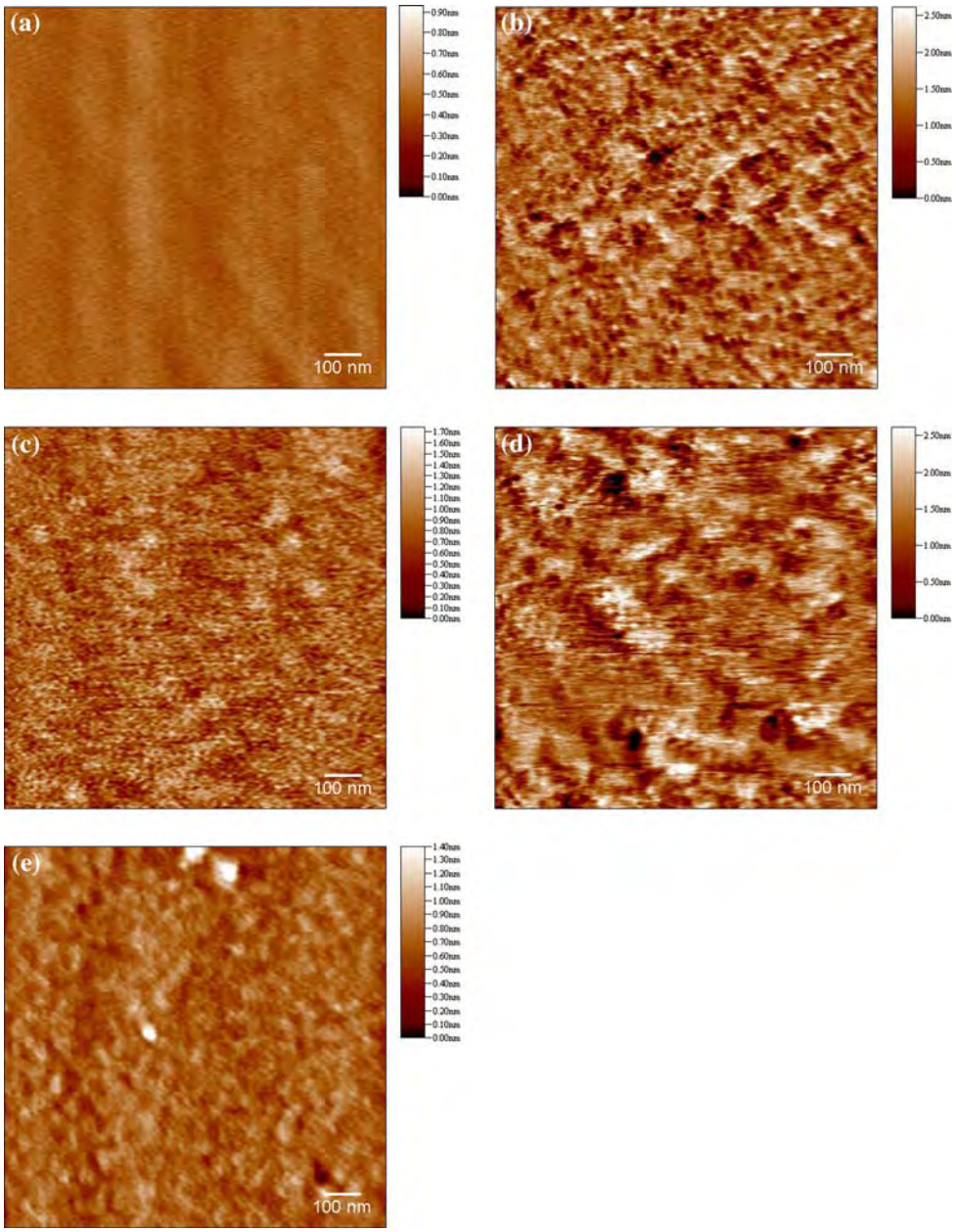

Fig. 6 AFM images for hydroxylated Si surface (**a**) and MIMCH-CL (**b**), MIMOH-CL (**c**), MIMCN-CL (**d**), and MIMCOOH-CL (**e**) film surfaces

The friction force is a lateral force exerted on a tip during scanning and can be measured using the twist of the tip/cantilever assembly. To obtain friction data, the tip was scanned back and forth in the x direction in contact with sample at a constant load while the lateral deflection of the lever was measured. The differences in the lateral deflection or friction signal between back and forth motions is proportional to the friction force. The friction force was calibrated by the method described in the reference [27]. Friction forces were continuously measured with various external loads. The load was increased (or decreased) linearly in each successive scan line. Scanning for the friction force measurement was performed at the rate of 1 Hz along the scan axis and a scan size of 50 × 50 μm^2 (viz. sliding velocity of 100 μm/s). The scan axis was perpendicular to the longitudinal direction of the cantilever. The sets of data were displayed graphically in a friction image.

2.3 Microscale Friction and Wear Measurements

Friction coefficient and durability at microscale were evaluated using a pin-on–plate tribometer in reciprocating mode. A Si_3N_4 ball of 3.18 mm diameter was fixed in a stationary holder sustained by a beam and the samples were then mounted on a reciprocating table. The ball moved horizontally with respect to the sample surface with sliding frequency between 1 and 4 Hz and a traveling distance of 5 mm. Applied normal loads used were between 60 and 400 mN and the change in friction coefficient was monitored versus sliding times or cycles. The initiation of wear on the sample surface leads to increase in friction coefficient, and a sharp increase indicates the failure of film. The friction coefficient and sliding cycles were recorded automatically by computer. A schematic illustration of pin-on-plate tribometer is showed in Fig. 3. All the tests were conducted at room temperature and a relative humidity of 15%.

The worn surfaces of the films were observed on a MicroXAM 3D non-contact interferometric microscope (ADE Phase Shift Inc, USA) with phase mode.

3 Results and Discussion

3.1 Characterization of Ionic Liquid and Films

The thermal properties of four kinds of ionic liquids were examined on a TGA-7 thermogravimetric analyzer (Perkin-Elmer, USA) between 20 °C and 600 °C with a heating rate of 10 °C min^{-1}. As shown in Fig. 4, all the ILs exhibited high decomposition temperature, and assigned to 275, 320, 263, and 270 °C, respectively.

Figure 5 shows the plots of film thickness as function of ionic liquids solution concentration. The data indicate that the linear increase in film thickness is associated with increase of the solution concentration. According to this relationship, a desired thickness of film was easily prepared.

Figure 6a–e shows AFM topographies for Si surface before and after dip-coating treatment in the ionic liquid solution. Figure 6a shows that hydroxylated Si surface is smooth and uniform with a root-mean-square (RMS) roughness of about 0.1 nm. The surface topographies of IMICH-CL, IMIOH-CL, IMICN-CL, and IMICOOH-CL ionic liquid films are shown in Fig. 6b–e, respectively. It is observed that the films were homogenously distributed on the silicon surface with the RMS roughness of about 0.41, 0.22, 0.46, and 0.12 nm, respectively.

3.2 Nanotribological Behavior

The adhesive forces between the AFM spherical tip and the IL film surfaces are shown in Fig. 7. Si substrate data are provided for comparison. Strong adhesive force was observed on the hydroxylated Si surface at humidity of 15%, on which the adhesive force was about 184 nN. After the ILs were coated, the adhesive forces were decreased to 121, 152, 136, and 138 nN, respectively. The adhesive force has been observed to decrease in the following order: MIMOH-CL > MIMCOOH-CL > MIMCN-CL > MIMCH-CL. The hydrophilic property of cationic end groups in IL films facilitated the formation of a meniscus, which increases the tip-sample adhesion. The adhesive force is lowest in MIMCH-CL since it has greatest amount of relative hydrophobic end groups among the four IL samples.

Figure 8 presents the plot of friction versus load curves for hydroxylated Si surface and the IL films. It is observed

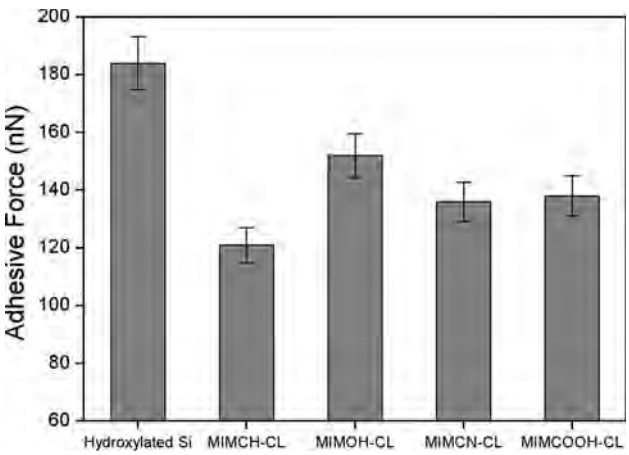

Fig. 7 Adhesive forces between colloidal probe and the surfaces of MIMCH-CL, MIMOH-CL, MIMCN-CL, and MIMCOOH-CL film at a humidity of 15%

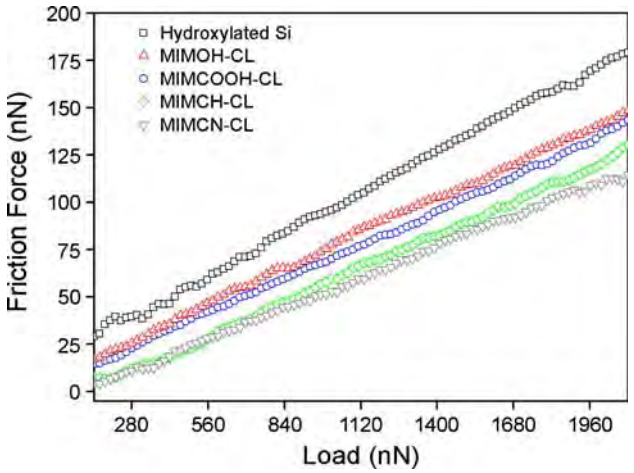

Fig. 8 Plot of friction and load for surfaces of the hydroxylated Si, MIMCH-CL, MIMOH-CL, MIMCN-CL, and MIMCOOH-CL at a humidity of 15%

that the IL films greatly reduced friction force, especially the MIMCH-CL and MIMCN-CL exhibited lowest friction. The results imply that the hydrophilic property of cationic end group samples facilitated sliding on the spherical tip on the surface. However, values of friction for MIMCOOH-CL and MIMOH-CL are higher than the data for MIMCH-CL and MIMCN-CL, as water and lubricant molecules are more likely to form a meniscus as the spherical tip approaches the surface. This provides greater resistance for tip sliding and leads to higher values of friction.

3.3 Microtribological Behavior

Tribological performance was evaluated for hydroxylated Si substrate and ionic liquid-coated surfaces with film thickness of about 2 nm. Without the protection of ionic liquid films, the coefficient of hydroxylated Si substrate

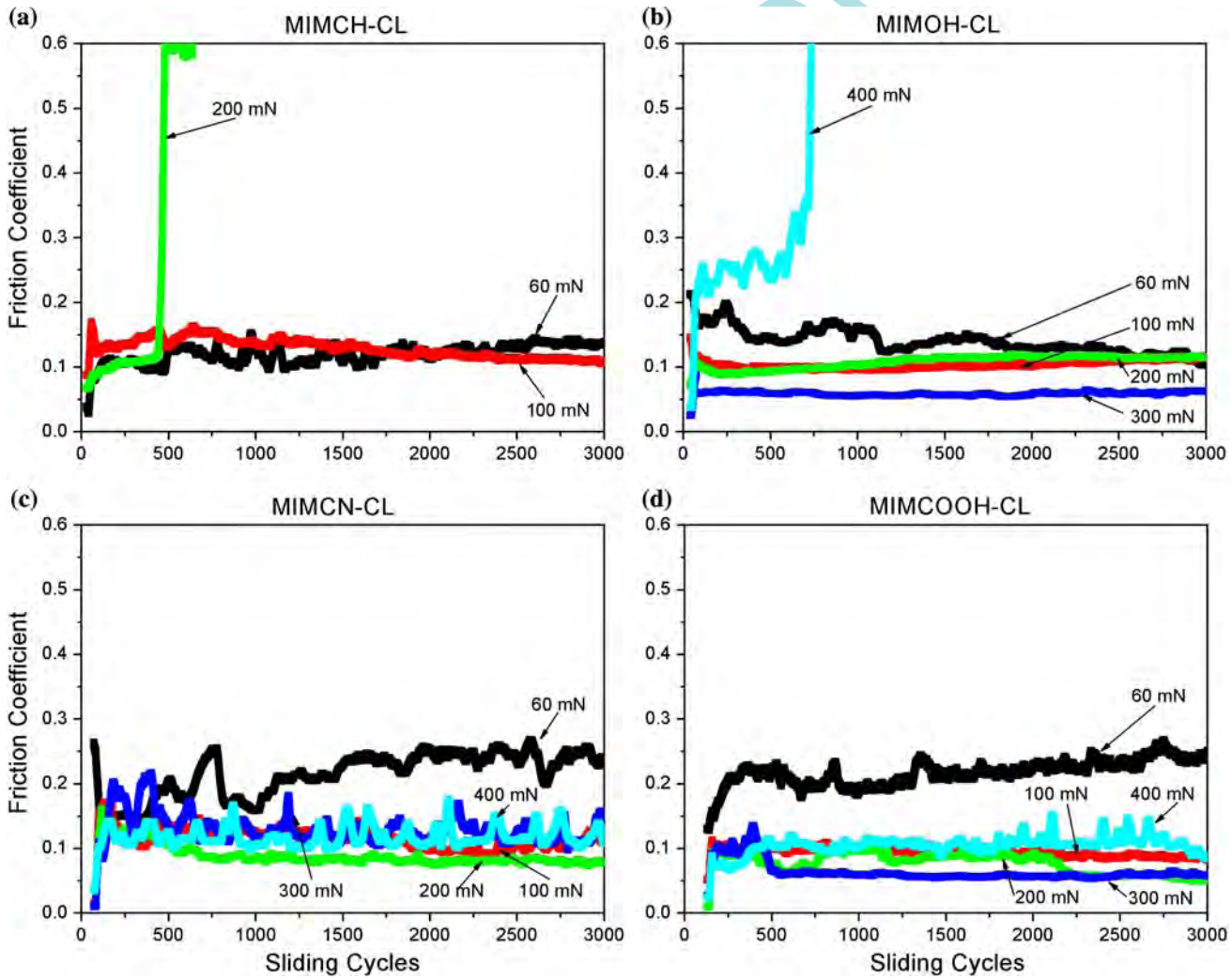

Fig. 9 Plot of friction coefficients as function of sliding cycles for MIMCH-CL (**a**), MIMOH-CL (**b**), MIMCN-CL (**c**), and MIMCOOH-CL (**d**) film on silicon

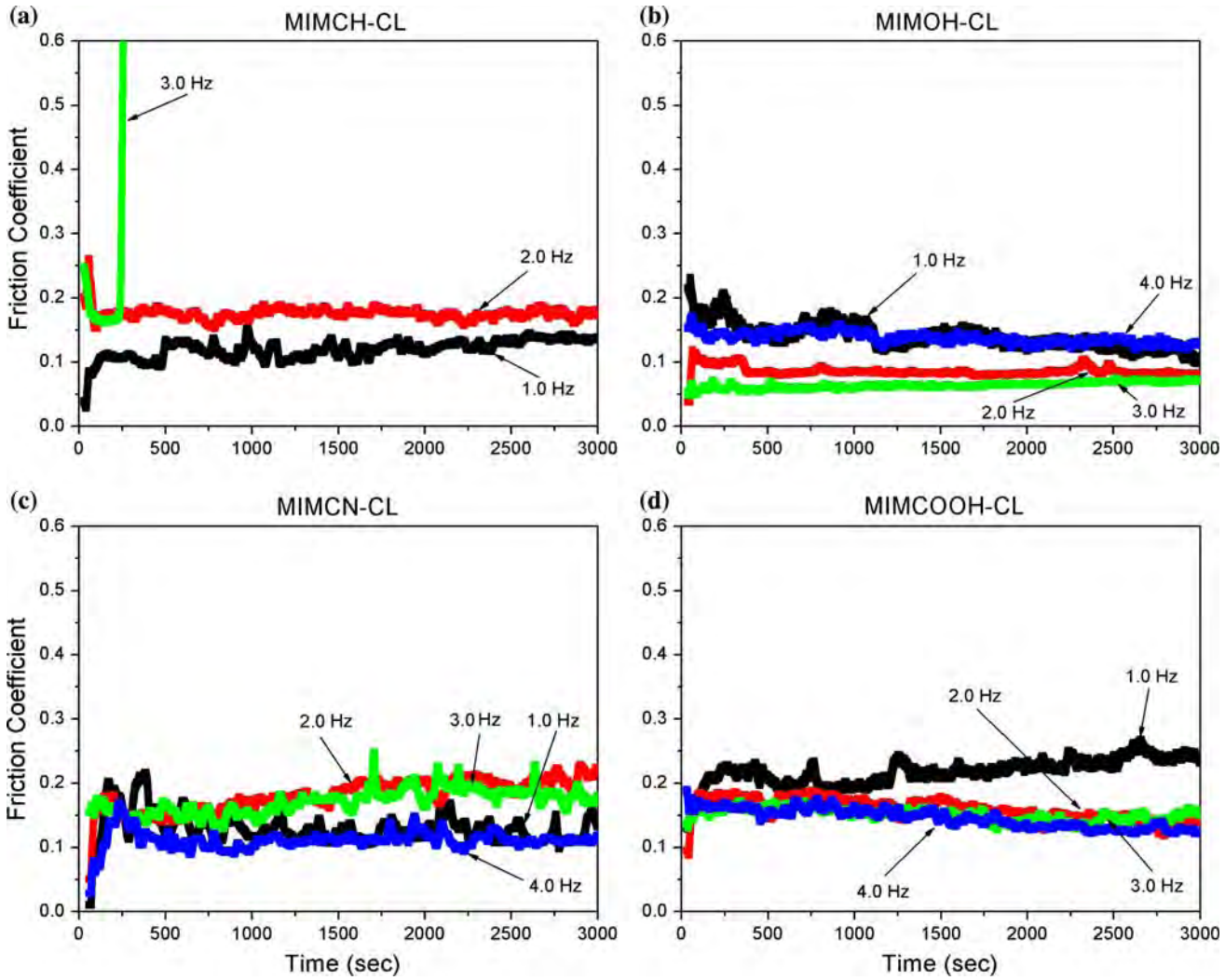

Fig. 10 Plot of friction coefficients as function of sliding frequency for MIMCH-CL (**a**), MIMOH-CL (**b**), MIMCN-CL (**c**), and MIMCOOH-CL (**d**) films at a normal load of 60 mN

increased sharply and was stable up to a constant value of about 0.65.

In order to compare friction and wear properties, conventional ball-on-plat tribometer experiments were conducted on the same samples. Figure 9a–d contains plots of the coefficient of friction as a function of the number of sliding cycles at normal loads range from 60 to 400 mN. As shown in Fig. 9a, the friction coefficients of MIMCH-CL were 0.12 and 0.09 at normal loads of 60 and 100 mN, respectively. When the normal load rose to 200 mN, the friction coefficient rose sharply over 0.6 before reaching 450 cycles, implying that the lubricant film failed. The friction coefficients of MIMOH-CL were averaged at 0.14, 0.10, 0.11, and 0.06 at normal loads of 60, 100, 200, and 300 mN, respectively as shown in Fig. 9b. The MIMOH film failed at normal load of 400 mN. As shown in Fig. 9c, d, the friction coefficients of MIMCN-CL and MIMCOOH-CL were averaged at 0.13 and 0.11 at all loads. Only a small rise in the coefficient of friction was observed for both MIMOH-CL and MIMCOOH-CL surface, indicating low surface wear. However, both MIMOH-CL and MIMCOOH-CL samples exhibited gradual change in value of friction coefficient. This is attributed to the transfer of lubricant molecules to the Si_3N_4 ball and the interaction of the transferred molecules with the lubricant still attached on the Si surface, which will increase the friction force.

Figure 10a–d shows the effect of sliding frequencies on coefficient of friction for all IL films at normal load of 60 mN. As shown in Fig. 10a, the friction coefficient of MIMCH-CL was averaged about 0.15 at relative mild condition (below 2 Hz). When the sliding frequency rose to 3 Hz, its friction coefficient sharply increased over 0.6 in several minutes, which indicated that the IL films failed completely under higher frequency reciprocating

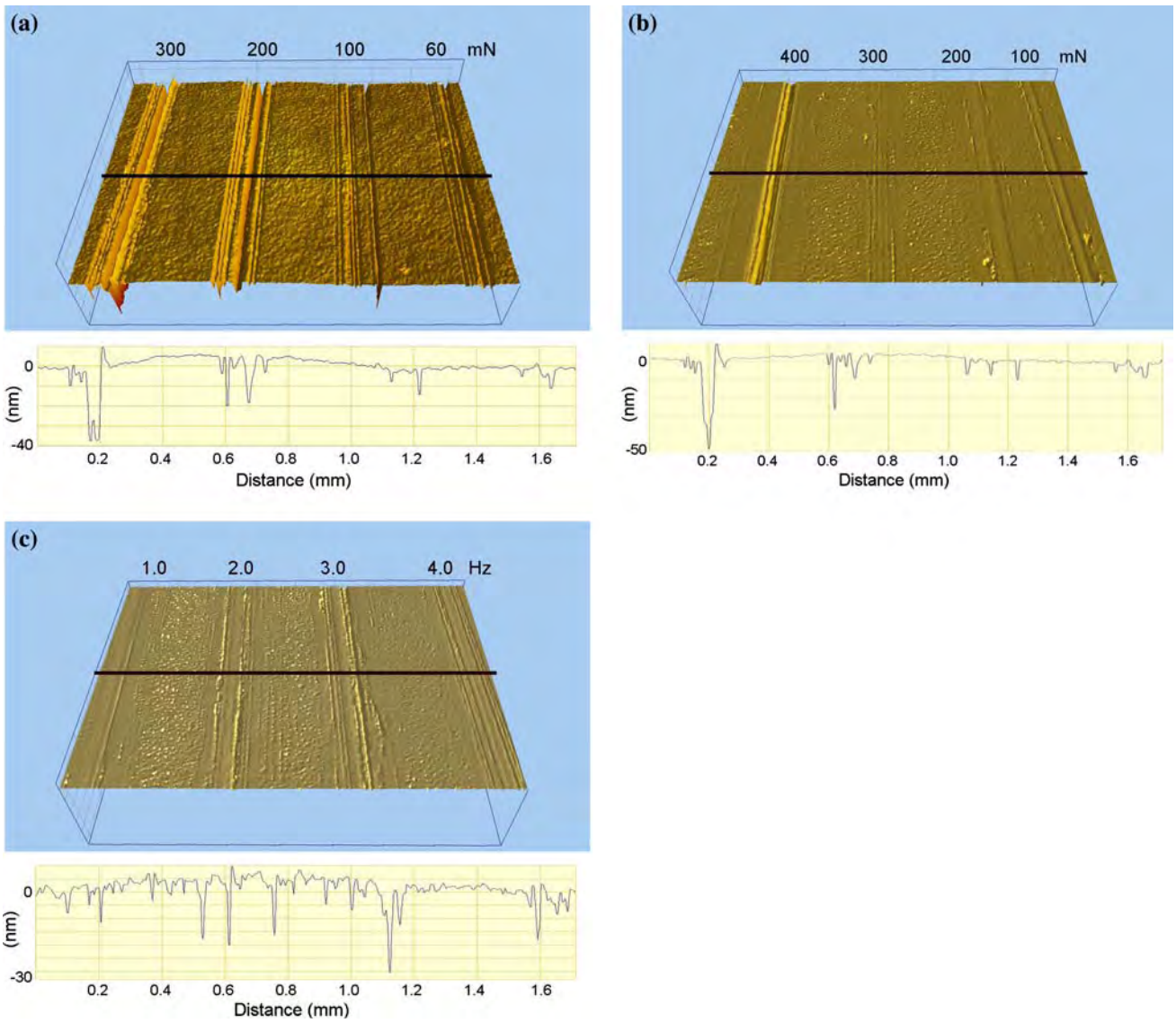

Fig. 11 3D interferometric microscope images and profiles of the wear tracks of MIMOH-CL film after sliding against a Si_3N_4 ball. **a** Hydroxylated Si at load range of 60–300 mN, frequency of 1 Hz for 100 cycles, **b** MIMOH-CL film at load range of 100–400 mN, frequency of 1 Hz for 3000 cycles, **c** MIMOH-CL film at frequency range of 1–4 Hz, load of 60 mN for 3,000 s

movement. At the same time, the MIMOH-CL, MIMCN-CL, and MIMCOOH still maintained low friction coefficients of 0.13, 0.11, and 0.14 under high frequency of 4 Hz, as shown in Fig. 10b–d. According this result, it is seen that the MIMOH-CL, MIMCN-CL, and MIMCOOH exhibit longer anti-wear durability under high frequency reciprocating slide, compared to the MIMCH-CL.

To further clarify the friction behavior, images and cross-section maps of wear tracks are shown in Fig. 11a–c. Figure 11a and b shows the worn surfaces of hydroxylated and IMIOH-CL-coated Si at various normal loads and a frequency of 1 Hz (viz. velocity of 10 mm/s) after sliding against the Si_3N_4 ball for 3,000 cycles. Figure 11c shows morphology of the worn surface of the MIMOH-CL-coated Si at various frequencies and normal load of 60 mN after sliding against the Si_3N_4 ball for 3,000 s. In all cases, a smaller amount of debris and slighter wear have been generated compared to the uncoated Si surface, indicating that the IL films provided wear protection. As shown in Fig. 11b and c, there exists obvious evidences of lubricant flowing back into the wear tracks, which did not occur in the uncoated Si (Fig. 11a). It is observed that some regions of the wear tracks were filled with lubricant, especially at lower loads and frequencies. The IL-coated Si exhibited low wear surfaces, which is attributed to lubricant replenishment by the mobile fraction.

4 Conclusions

This study has demonstrated that four kinds of ionic liquid films with thickness ranging from approximately 2 to 60 nm were prepared as uniform coatings by dip-coating method. Adhesion and friction experiments at nanoscale were carried out using a colloidal probe. Based on topography adhesion and friction data, all IL films are prone to attach to the silicon substrate surface, leading to more uniform coatings and lowered adhesion and friction. The MIMCN-CL and MIMCH-CL show favorable lubrication, as seen from the adhesion and friction being less than that of MIMOH-CL, MIMCOOH-CL, and uncoated silicon in all cases. The microscale friction and wear of the four ionic liquid films were evaluated at load range of 60–400 mN and the sliding frequency range of 1–4 Hz. All ionic liquids show favorable friction reduction and durability. MIMCN-CL and MIMCOOH-CL exhibited low friction coefficient and long durability even at a normal load of 400 mN. The MIMOH-CL, MIMCN-CL, and MIMCOOH-CL exhibited lower friction and better anti-wear durability at high frequency sliding (4 Hz) compared with MIMCH-CL in microscale. Thus, from a tribological point of view, the ionic liquids show strong potential as lubricant for MEMS because they have desirable thermal and tribological properties.

Acknowledgment This work was funded by National Natural Science Foundation of China (NSFC) under Grant Number 50675217 and National 973 Program: 2007CB607601.

References

1. Spearing, S.M.: Materials issues in microelectromechanical systems (MEMS). Acta Mater. **48**, 179–196 (2000). doi:10.1016/S1359-6454(99)00294-3
2. Bhushan, B.: Springer Handbook of Nanotribology of Nanotechnology, 2nd edn. Springerverlag, Heidelberg, Germany (2007)
3. Sulouffin, R.E., Bhushan, B.: Tribology Issue and Opportunities in MEMS, pp. 109–119. Kluwer Academic, Dordrecht (1998)
4. Liu, H., Bhushan, B.: Investigation of nanotribological and nanomechanical properties of the digital micromirror device by atomic force microscopy. J. Vac. Sci. Technol. A **22**, 1388–1396 (2004). doi:10.1116/1.1743050
5. Liu, H., Bhushan, B.: Investigation of nanotribological properties of self-assembled monolayers with alkyl and biphenyl space chains. Ultramicroscopy **91**, 185–202 (2002). doi:10.1016/S0304-3991(02)00099-2
6. Welton, T.: Room temperature ionic liquids: solvents for synthesis and catalysis. Chem. Rev. **9**, 2071–2083 (2005)
7. Wasserscheid, P., Keim, W.: Ionic liquids—new "solutions" for transition metal catalysis. Chem. Int. Ed. **39**, 3772–3789 (2000)
8. Huddleston, J.G., Visser, A.E., Reichert, W.M., Willauer, H.D., Broker, G.A., Roger, R.D.: Characterization and comparison of hydrophilic and hydrophobic room temperature ionic liquids incorporating the imidazolium cation. Green Chem. **3**, 156–164 (2001). doi:10.1039/b103275p
9. Dupont, J., Souza, R.F., Suarez, P.A.Z.: Ionic liquid (molten salt) phase organometallic catalysis. Chem. Rev. **102**, 3667–3692 (2002). doi:10.1021/cr010338r
10. Roger, R.D., Seddon, K.R.: Ionic Liquids: Industrial Applications for Green Chemistry. ACS Symposium Series 818 American Chemical Society, Washington, DC (2002)
11. Ye, C.F., Liu, W.M., Chen, Y.X., Yu, L.G.: Room temperature ionic liquids: a kind of novel versatile lubricant. Chem. Commun. **1**, 2244–2245 (2001). doi:10.1039/b106935g
12. Liu, X., Zhou, F., Liang, Y., Liu, W.: Benzotriazole as the additive for ionic liquid lubricant: one pathway towards actual application of ionic liquids. Tribol. Lett. **23**, 191–196 (2006). doi:10.1007/s11249-006-9050-7
13. Xia, Y.Q., Sasaki, S., Murakami, T., Nakano, M., Shi, L., Wang, H.Z.: Ionic liquid lubrication of electrodeposited nickel–Si_3N_4 composite coatings. Wear **262**, 765–771 (2007). doi:10.1016/j.wear.2006.06.015
14. Bonhote, P., Dias, A., Papageoriou, N., Kalyanasundaram, K., Gratzel, M.: Hydrophobic, highly conductive ambient-temperature molten salts. Inorg. Chem. **35**, 1168–1178 (1996). doi:10.1021/ic951325x
15. Qu, J., Truhan, J.J., Dai, S., Luo, H., Blau, P.J.: Ionic liquids with ammonium cations as lubricants or additives. Tribol. Lett. **22**, 207–214 (2006). doi:10.1007/s11249-006-9081-0
16. Liu, X.Q., Zhou, F., Liang, Y.M., Liu, W.M.: Tribological performance of phosphonium based ionic liquids for an aluminum-on-steel system and opinions on lubrication mechanism. Wear **261**, 1174–1179 (2006). doi:10.1016/j.wear.2006.03.018
17. Jimenez, A.E., Bernudez, M.D., Carrion, F.J., Nicolas, G.M.: Room temperature ionic liquids as lubricant additives in steel-aluminium contact: influence of sliding velocity, normal load and temperature. Wear **261**, 347–359 (2006). doi:10.1016/j.wear.2005.11.004
18. Liu, W.M., Ye, C.F., Gong, Q.Y., Wang, H.Z., Wang, P.: Tribological performance of room-temperature ionic liquids as lubricant. Tribol. Lett. **13**, 81–85 (2002). doi:10.1023/A:1020148514877
19. Bhushan, B., Palacio, M., Kinzig, B.: AFM-based nanotribological and electrical characterization of ultrathin wear-resistant ionic liquid films. J. Colloid Interface Sci. **317**, 275–287 (2008). doi:10.1016/j.jcis.2007.09.046
20. Van Valkenburg, M.E., Vaughn, R.L., Williams, M., Wikes, J.S.: Thermochemistry of ionic liquid heat-transfer fluids. Thermochim. Acta **425**, 181–188 (2005). doi:10.1016/j.tca.2004.11.013
21. Tao, Z., Bhushan, B.: Bonding, degradation, and environmental effects on novel perfluoropolyether lubricants. Wear **259**, 1352–1361 (2005). doi:10.1016/j.wear.2005.01.013
22. Caporiccio, G., Flabbi, L., Marchionniand, G., Viola, G.T.: The properties and applications of perfluoropolyether lubricants. J Synth Lubr **6**, 133–149 (1989). doi:10.1002/jsl.3000060205
23. Mori, S., Morales, W.: Tribological reactions of perfluoroalkyl polyether oils with stainless steel under ultrahigh vacuum conditions at room temperature. Wear **132**, 111–121 (1989). doi:10.1016/0043-1648(89)90206-8
24. Bo, Y., Zhou, F., Mu, Z.G., Liang, Y.M., Liu, W.M.: Tribological properties of ultra-thin ionic liquid films on single-crystal silicon wafers with functionalized surfaces. Tribol Int. **39**, 879–887 (2006). doi:10.1016/j.triboint.2005.07.039
25. Tsukruk, V.V., Bliznyuk, V.N.: Adhesive and friction forces between chemically modified silicon and silicon nitride surfaces. Langmuir **14**, 446–455 (1998). doi:10.1021/la970367q
26. Xiao, X.D., Qian, L.M.: Investigation of humidity-dependent capillary force. Langmuir **16**, 8153–8158 (2000). doi:10.1021/la000770o
27. Bhushan, B.: Handbook of Micro/Nano Tribology, 2nd edn. CRC Press, Boca Raton, FL (1994)